PHYSICAL REVIEW B **70**, 140501(R) (2004)

# Entangling flux qubits with a bipolar dynamic inductance

B. L. T. Plourde,[1] J. Zhang,[2,3] K. B. Whaley,[3] F. K. Wilhelm,[4] T. L. Robertson,[4] T. Hime, S. Linzen,[1] P. A. Reichardt,[1] C.-E. Wu,[1] and John Clarke[1]

[1]*Department of Physics, University of California, Berkeley, California 94720, USA*

[2]*Department of Electrical Engineering and Computer Sciences, University of California, Berkeley, California 94720, USA*

[3]*Department of Chemistry, University of California, Berkeley, California 94720, USA*

[4]*Department Physik and CeNS, Ludwig-Maximilians-Universität, Theresienstr. 37, 80333 München, Germany*

(Received 4 May 2004; published 5 October 2004)

We propose a scheme to implement controllable coupling between two flux qubits using the screening current response of a dc superconducting quantum interference device (SQUID). The coupling strength is adjusted by the current bias applied to the SQUID and can be varied continuously from positive to negative values, allowing cancellation of the direct mutual inductance between the qubits. We show that this variable coupling scheme permits efficient realization of universal quantum logic. The same SQUID can be used to determine the flux states of the qubits.

DOI: 10.1103/PhysRevB.70.140501 PACS number(s): 85.25.Cp, 03.67.Lx, 85.25.Dq

A rich variety of quantum bits (qubits) is being explored for possible implementation in a future quantum computer.[1] Of these, solid-state qubits are attractive because of their inherent scalability using well-established microfabrication techniques. A subset of these qubits is superconducting, and includes devices based on charge,[2,3] magnetic flux,[4–6] and the phase difference[7] across a Josephson junction. To implement a quantum algorithm, one must be able to entangle multiple qubits, so that an interaction term is required in the Hamiltonian describing a two-qubit system.[8] For two superconducting flux qubits, the natural interaction is between the magnetic fluxes. Placing the two qubits in proximity provides a permanent coupling through their mutual inductance.[9] Pulse sequences for generating entanglement have been derived for several superconducting qubits with fixed interaction energies.[10,11] However, entangling operations can be much more efficient if the interaction can be varied and, ideally, turned off during parts of the manipulation. A variable coupling scheme for charge-based superconducting qubits with a bipolar interaction has been suggested recently.[12] For flux qubits, while switchable couplings have been proposed previously,[13,14] these approaches do not enable one to turn off the coupling entirely or require separate coupling and flux readout devices.

In this communication, we propose a coupling scheme for flux qubits in which the interaction is adjusted by changing a small current. For suitable device parameters the *sign* of the coupling can be changed, making it possible to null out the direct interaction between the qubits. Furthermore, the same device can be used both to vary the coupling and to read out the flux states of the qubits. We show explicitly how this variable qubit coupling can be combined with microwave pulses to perform the quantum controlled-NOT (CNOT) logic gate. Using microwave pulses also for arbitrary single-qubit operations, this scheme provides all the necessary ingredients to implement scalable universal quantum logic.

The coupling is mediated by the circulating current $J$ in a dc superconducting quantum interference device (SQUID), in the zero-voltage state, which is coupled to each of two qubits through an identical mutual inductance $M_{qs}$ [Fig. 1(a)]. The SQUID consists of two Josephson junctions, each with capacitance $C$ and critical current $I_0$ at $T=0$, on a superconducting loop of inductance $L$. The dynamics of the SQUID are described by the phase difference across each junction $\gamma_{1,2}$.[15] A variation in the flux applied to the SQUID, $\Phi_s$, changes $J$ and $I_c$, the critical current at which the SQUID switches out of the zero-voltage state in the absence of quantum tunneling [Fig. 1(b)]. The response is governed by the screening parameter $\beta_L \equiv 2LI_0/\Phi_0$ and the externally controlled bias current $I_b < I_c(\Phi_s)$. In flux qubit experiments,[16] the flux state is determined by a SQUID to which fast pulses of $I_b$ are applied to measure $I_c(\Phi_s, T)$. Thus, existing technology allows $I_b$ to be varied rapidly, and a single SQUID can be used both to measure the two qubits and to couple them together controllably.

The flux qubit consists of a superconducting loop interrupted by three Josephson junctions.[4,13] With a flux bias near the degeneracy point, $\Phi_0/2$, a screening current $I_q$ can flow in either direction around the loop. Given the tunnel coupling energy $\delta$ between the different directions of $I_q$, the ground and first excited states of the qubit correspond to symmetric and antisymmetric superpositions of these two current states.

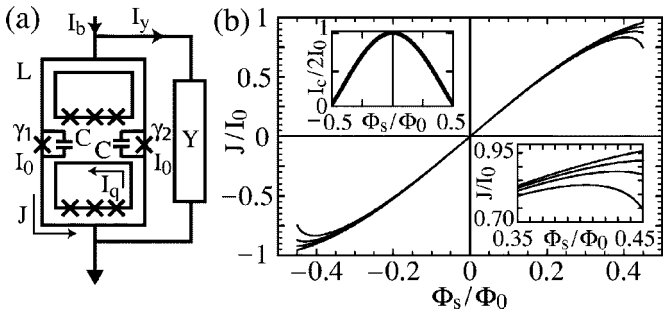


FIG. 1. (a) SQUID-based coupling scheme. The admittance $Y$ represents the SQUID bias circuitry. (b) Response of SQUID circulating current $J$ to applied flux $\Phi_s$ for $\beta_L=0.092$ and $I_b/I_c(0.45\Phi_0)=0, 0.4, 0.6, 0.85$ (top to bottom). The lower right inset shows $J(\Phi_s)$ for same values of $I_b$ near $\Phi_s=0.45\Phi_0$. The upper left inset shows $I_c$ vs $\Phi_s$.

 

Thus, the dynamics of qubit $i$ can be approximated by the Hamiltonian

$$\mathcal{H}_i = -(\epsilon_i^0/2)\sigma_z^{(i)} - (\delta_i/2)\sigma_x^{(i)}. \quad (1)$$

The energy biases $\epsilon_i^0$ are determined by the flux bias of each qubit relative to $\Phi_0/2$. The tunnel frequencies $\delta_i/h$ are fixed by the device parameters and are typically a few GHz. For two flux qubits, arranged so that a flux change in one qubit alters the flux in the other, the coupled-qubit Hamiltonian describing the dynamics in the complex four-dimensional Hilbert space becomes

$$\mathcal{H} = \mathcal{H}_1 \otimes I^{(2)} + I^{(1)} \otimes \mathcal{H}_2 - (K/2)\sigma_z^{(1)} \otimes \sigma_z^{(2)}, \quad (2)$$

where $I^{(i)}$ is the identity matrix for qubit $i$ and $K$ characterizes the coupling energy. For $K<0$, the minimum-energy configuration corresponds to antiparallel fluxes. For two flux qubits coupled through a mutual inductance $M_{qq}$, the interaction energy is fixed at $K_0=-2M_{qq}|I_q^{(1)}||I_q^{(2)}|$.

In addition to the direct coupling, $K_0$, the qubits interact by changing the current $J$. The response of $J$ to a flux change depends strongly on $I_b$ [Fig. 1(b)]. When $I_q^{(2)}$ switches direction, the flux coupled to the SQUID, $\Delta\Phi_s^{(2)}$, induces a change $\Delta J$ in the circulating current in the SQUID, and alters the flux coupled from the SQUID to qubit 1. The corresponding coupling is

$$\begin{aligned} K_s &= |I_q^{(1)}|\Delta\Phi_q^{(1)} = |I_q^{(1)}|M_{qs}\Delta J, \\ &= |I_q^{(1)}|M_{qs}\mathrm{Re}(\partial J/\partial\Phi_s)_{I_b}\Delta\Phi_s^{(2)}, \\ &= -2M_{qs}^2|I_q^{(1)}||I_q^{(2)}|\mathrm{Re}(\partial J/\partial\Phi_s)_{I_b}. \end{aligned} \quad (3)$$

The transfer function, $(\partial J/\partial\Phi_s)_{I_b}$, is related to the dynamic impedance, $\mathcal{Z}$, of the SQUID via[17]

$$\partial J/\partial\Phi_s = i\omega/\mathcal{Z} = 1/\mathcal{L} + i\omega/\mathcal{R}, \quad (4)$$

where $\mathcal{R}$ is the dynamic resistance, determined by $Y$, which dominates any loss in the junctions, and $\mathcal{L}$ is the dynamic inductance which, in general, differs from $L$.

We evaluate $(\partial J/\partial\Phi_s)_{I_b}$ by current conservation, neglecting currents flowing through the junction resistances,

$$I_b = I_y + 2I_0 \cos\Delta\gamma \sin\overline{\gamma} + 2C(\Phi_0/2\pi)\ddot{\overline{\gamma}}, \quad (5)$$

$$J = I_0 \cos\overline{\gamma}\sin\Delta\gamma + C(\Phi_0/2\pi)\Delta\ddot{\gamma}. \quad (6)$$

Here, $I_y$ is the current flowing through the admittance $Y(\omega)$ [Fig. 1(a)]. Equations (5) and (6) describe the dynamics of $\gamma_{1,2}$ through the variables $\Delta\gamma=(\gamma_1-\gamma_2)/2$ and $\overline{\gamma}=(\gamma_1+\gamma_2)/2$; $\gamma_1$ and $\gamma_2$ are constrained by $d\Delta\gamma=(\pi/\Phi_0)(d\Phi_s - LdJ)$.

The expression for $K_s$ in terms of $\mathrm{Re}(\partial J/\partial\Phi_s)_{I_b}$ [Eq. (3)] requires the qubit frequencies to be much lower than the characteristic frequencies of the SQUID, thus ensuring that the SQUID stays in its ground state during qubit entangling operations. Furthermore, it is a reasonable approximation to take the $\omega=0$ limit of $\mathrm{Re}(\partial J/\partial\Phi_s)_{I_b}$ to calculate $K_s$, so that we can solve Eqs. (5) and (6) numerically to obtain the working point; for the moment we assume $Y(0)=0$. For the small deviations determining $K_s$, we linearize Eqs. (5) and (6) and solve for the real part of the transfer function in the low-frequency limit,

$$\mathrm{Re}\left(\frac{\partial J}{\partial\Phi_s}\right)_{I_b} = \frac{1}{2L_j}\frac{1-\tan^2\Delta\gamma\tan^2\overline{\gamma}}{1+\frac{L}{2L_j}(1-\tan^2\Delta\gamma\tan^2\overline{\gamma})}. \quad (7)$$

Here, we have introduced the Josephson inductance for one junction, $L_j=\Phi_0/2\pi I_0\cos\Delta\gamma\cos\overline{\gamma}$. For $\beta_L\gg1$, Eq. (7) approaches $1/L$, while for $\beta_L\ll1$,

$$\mathrm{Re}(\partial J/\partial\Phi_s)_{I_b} = (1/2L_j)(1-\tan^2\Delta\gamma\tan^2\overline{\gamma}). \quad (8)$$

We see that $\mathrm{Re}(\partial J/\partial\Phi_s)_{I_b}$ is negative for sufficiently high values of $I_b$ and $\Phi_s$, which increase $\overline{\gamma}$ and $\Delta\gamma$, as shown by the dependence of $J(\Phi_s)$ on $I_b$ in Fig. 1(b).

We choose the SQUID parameters $L=200$ pH, $C=5$ fF, and $I_0=0.48$ $\mu$A, for which $\beta_L=0.092$. The qubits are characterized by $|I_q^{(1)}|=|I_q^{(2)}|=0.46$ $\mu$A, $M_{qs}=33$ pH, and $M_{qq}=0.25$ pH, yielding $K_0/h=-0.16$ GHz. If we choose $\Phi_s=0.45\Phi_0$, Eqs. (3) and (7) result in a net coupling strength $K/h=(K_0+K_s)/h$, that is $-0.3$ GHz when $I_b=0$, and $K=0$ when $I_b/I_c(0.45\Phi_0)=0.57$ [Fig. 2(a)]. By solving Eqs. (5) and (6) before taking the $\omega=0$ limit, we find that the lowest-frequency mode of the SQUID with $I_b/I_c(0.45\Phi_0)=0.57$ occurs near 44 GHz, much higher than the qubit energy splittings, $\Delta E_i$, of about 10 GHz. Thus, our zero-frequency approximation in Eqs. (7) and (8) is justified. The change in sign of $K_s$ does not occur for all $\beta_L$. Figure 2(b) shows the highest achievable value of $K_s$ versus $\beta_L$. We have adopted the optimal design at $\beta_L=0.092$.

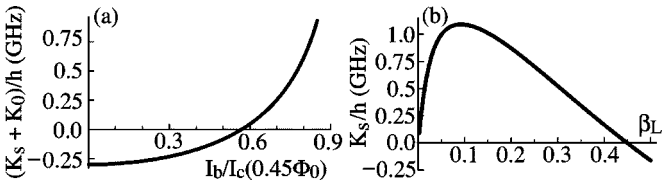


FIG. 2. (a) Variation of $K$ with $I_b$ for $\Phi_s=0.45\Phi_0$ and device parameters described in the text. (b) Highest achievable value of $K_s$ vs $\beta_L$ evaluated at $I_b=0.85I_c(0.45\Phi_0)$; $I_0$ (and hence $\beta_L$) is varied for $L=200$ pH.

We also need to consider crosstalk between the coupling and single-qubit terms in the Hamiltonian. When the coupling is switched, in addition to $\partial J/\partial\Phi_s$ being altered, $J$ also changes, thus shifting the flux biases of the qubits. The calculated change in $J$ as the coupler is switched from $I_b=0$ to $I_b/I_c(0.45\Phi_0)=0.57$ produces a change in the flux in each qubit corresponding to an energy shift $\delta\epsilon_1/h=\delta\epsilon_2/h=1.64$ GHz. In addition, when the qubits are driven by microwaves to produce single-qubit rotations, the microwave flux may also couple to $\Phi_s$. As a result, $K$ is weakly modulated when the coupling would nominally be turned off. A typical microwave drive $\tilde{\epsilon}_i(t)/h$ of amplitude 1 GHz results in a variation of about $\pm14$ MHz about $K=0$.

When the bias current is increased to switch off the coupling, the SQUID symmetry is broken and the qubits are

coupled to the noise generated by the admittance $Y$. We estimate the decoherence due to this process by calculating the environmental spectral density $\mathcal{J}(\omega)$ in the spin-boson model.[18] We obtain $\mathcal{J}(\omega)$ from the classical equation of motion for the qubit flux with the dissipation from $Y$ coupled to either qubit through $J$,

$$\mathcal{J}(\omega) = (I_q^2 M_{qs}^2/h)\mathrm{Im}(\partial J/\partial \Phi_s)_{I_b}. \quad (9)$$

To calculate $\mathcal{J}(\omega)$, we linearize Eqs. (5) and (6) around the equilibrium point to obtain

$$d\overline{\gamma} = \frac{2\tan\overline{\gamma}\tan\Delta\gamma}{L_j}\frac{1}{2/L_j - 2\omega^2 C + i\omega Y}d\Delta\gamma. \quad (10)$$

For the case $Y^{-1}=R$, following the path to the static transfer function Eq. (7) and taking the imaginary part in the low-$\beta_L$ limit, we obtain $\mathrm{Im}(\partial J/\partial\Phi_s)_{I_b} = -\omega/\mathcal{R} = (\omega/4R)\tan^2\Delta\gamma\tan^2\overline{\gamma}$. Thus $\mathcal{J}(\omega)=\alpha\omega$, where $\alpha = (M_{qs}^2 I_q^2/4hR)\tan^2\Delta\gamma\tan^2\overline{\gamma}$, and $\alpha(I_b=0)=0$. As $I_b$ is increased to change the coupling strength, $\alpha$ increases monotonically. For the parameters above and $R=2.4$ k$\Omega$, when the net coupling is zero [ $I_b/I_c(0.45\Phi_0)=0.57$, Fig. 2(a)] we find $\alpha \approx 8\times 10^{-5}$, corresponding to a dephasing time $\approx$500 ns, an order of magnitude larger than current experimental values.[16]

We now show that this configuration implements universal quantum logic efficiently. Any $n$-qubit quantum operation can be decomposed into combinations of two-qubit entangling gates, for example, CNOT, and single-qubit gates.[19] Two-qubit gates which cannot be decomposed into a product of single-qubit gates are said to be nonlocal, and may lead to entanglement between the two qubits.[20] Since we can adjust the qubit coupling $K$ to zero, we can readily implement single-qubit gates with microwave pulses as described below.

To implement the nonlocal two-qubit CNOT gate, we use the concept of local equivalence: the two-qubit gates $U_1$ and $U_2$ are locally equivalent if $U_1 = k_1 U_2 k_2$, where $k_1$ and $k_2$ are local two-qubit gates which are combinations of single-qubit gates applied simultaneously. The local gate which precedes $U_2$, $k_2$, is given by $k_{21}\otimes k_{22}$, where $k_{21(22)}$ is a single-qubit gate for qubit 1(2), while the local gate which follows $U_2$, $k_1$, is $k_{11}\otimes k_{12}$, where $k_{11(12)}$ is a single-qubit gate for qubit 1(2).[21] Our strategy is to find efficient implementation of a nonlocal quantum gate $U_2$ that differs only by local gates, $k_1$ and $k_2$, from CNOT, using the methods in Ref. 20 and then to add those local operations required to achieve a CNOT gate in the computational basis, in which the SQUID measures the projection of each qubit state vector onto the $z$-axis.

The local equivalence classes of two-qubit operations are in one-to-one correspondence with points in a tetrahedron, the Weyl chamber.[20] In this representation, any two-qubit operation is associated with the point $[c_1,c_2,c_3]$, where CNOT corresponds to $[\pi/2,0,0]$. Furthermore, the nonlocal two-qubit gates generated by a Hamiltonian acting for time $t$ can be mapped to a trajectory in this space.[16] If $I_b$ is varied such that $K$ is increased instantaneously to a constant value, the trajectory generated by Eq. (2) is well described by the periodic curve

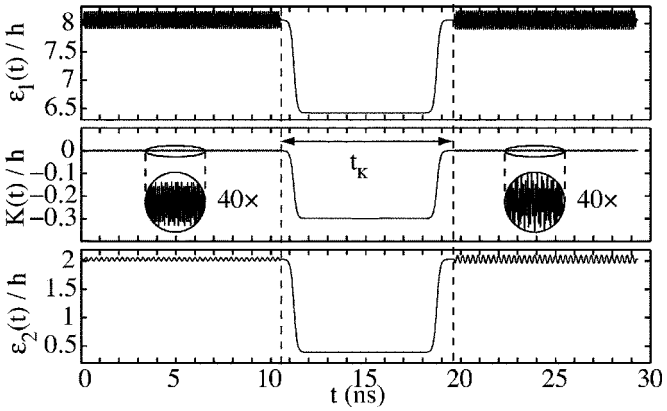


FIG. 3. Pulse sequence for implementing CNOT gate. Energy scales in GHz. Total single-qubit energy bias $\epsilon_i(t) = \epsilon_i^0 + \tilde{\epsilon}_i(t) + \delta\epsilon_i(t)$, where microwave pulses $\tilde{\epsilon}_{1,2}(t)$ produce single-qubit rotations in the decoupled configuration; crosstalk modulation of $K(t)$ is shown (see text). The bias current is pulsed to turn on the interaction in the central region.

$$[c_1,c_2,c_3] = [Kvt/\hbar, p|\sin\omega t|, p|\sin\omega t|]. \quad (11)$$

Here, $p$ is a function of the system parameters, $v = \epsilon_1^0\epsilon_2^0/\Delta E_1\Delta E_2$, and $\omega = (\Delta E_1 - \Delta E_2)/2\hbar$, where $\Delta E_i = [(\epsilon_i^0)^2 + \delta_i^2]^{1/2}$ is the single-qubit energy-level splitting. Independently of $p$, this trajectory reaches $[\pi/2,0,0]$ in a time $t_K = n\pi/\omega$ when the coupling strength is tuned to $K = \hbar\omega/2nv$, with $n$ a nonzero integer.

While this analytic solution contains the essential physics, it does not include vital experimental features, in particular, crosstalk and the finite rise time of the bias current pulse. To improve the accuracy, we perform a numerical optimization using Eq. (11) as a starting point, then add these corrections. We set $\delta_1/h = 5$ GHz and $\delta_2/h = 3$ GHz, and include the shifts of the single-qubit energy biases due to the crosstalk with $K_s$ in Eq. (11) by adding a shift $\delta\epsilon_i$ proportional to $K$. We account for the rise and fall times of the current pulse by using pulse edges with 90% widths of 0.5 ns [see $K(t)$ in Fig. 3]. We numerically optimize the variable parameters to minimize the Euclidean distance between the actual achieved gate and the desired Weyl chamber target CNOT gate. If $I_b$ is pulsed to provide $K/h = -0.30$ GHz for a time $t_K = 8.74$ ns, we find that the gate locally equivalent to CNOT is reached when the externally controlled static flux biases are set to yield $\epsilon_1^0/h = 8.06$ GHz and $\epsilon_2^0/h = 2.03$ GHz throughout the operation.

As outlined above, to achieve a true CNOT gate we still have to determine the pulse sequences which implement the requisite local gates that take this Weyl chamber target $U_2$ to CNOT in the computational basis. Local gates may be implemented by applying microwave radiation, $\tilde{\epsilon}_i(t)$, which couples to $\sigma_z^{(i)}$, and is at or near resonance with the single-qubit energy-level splitting $\Delta E_i$. To simplify the pulse sequence, we keep $\epsilon_{1,2}^0$ constant at the values used for the nonlocal gate generation. This imposes an additional constraint on the local gates: to generate a local two-qubit gate $k_1 = k_{11}\otimes k_{12}$, the two single-qubit gates $k_{11}$ and $k_{12}$ must be simultaneous and of equal duration. We satisfy this constraint

by making the microwave pulse addressing one-qubit resonant and that addressing the other slightly off resonance. Using this offset and the relative amplitude and phase of the two microwave pulses as variables, we can achieve two different single-qubit gates simultaneously, leading to our required local two-qubit gate.

The resulting pulse sequences for $K$ and $\tilde{\epsilon}_{1,2}$ are shown in Fig. 3. The static flux biases which determine $\epsilon_{1,2}^0$ remain fixed throughout the entire pulse sequence and are chosen to provide a large frequency separation between $\Delta E_1/h$ and $\Delta E_2/h$. This ensures that the microwave radiation to produce the single-qubit gate for qubit 1 is far off resonance for qubit 2. This constraint could be relaxed if one could engineer the microwave driving with two separate antennas, each one coupling selectively to one of the qubits. The gate has a maximum deviation from CNOT in the computational basis of 0.016 in any matrix element. This error arises predominantly from the single microwave antenna which leads to cross coupling of the microwave signals for the two qubits and the weak modulation of the $K=0$ state of the coupler during the single-qubit microwave manipulations. While small, this error could be reduced further by performing the numerical optimization with higher precision or by coupling the microwave flux selectively to each qubit and not to the SQUID. The total elapsed time of 29.35 ns is comparable to measured dephasing times in a single flux qubit.[19]

In summary, we have shown that the inverse dynamic inductance of a dc SQUID with low $\beta_L$ in the zero-voltage state can be controlled by bias current pulses. This technique provides a variable strength interaction $K_s$ between flux qubits coupled to the SQUID, and enables cancellation of the direct mutual inductive coupling $K_0$ between the qubits so that the net coupling $K$ can be switched to zero. By steering a nonlocal gate trajectory and combining it with local gates composed of simultaneous single-qubit rotations driven by resonant and off-resonant microwave pulses, we have shown that a simple pulse sequence containing a single switching of the flux coupling for fixed static flux biases results in a CNOT gate and full entanglement of two flux qubits. Furthermore, the same SQUID can be used to determine the flux state of the qubits. This approach should be scalable to larger numbers of qubits, as, for example, in Fig. 4.

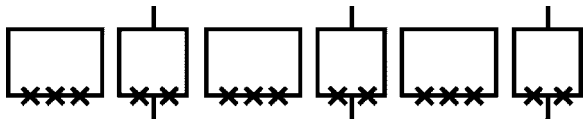

FIG. 4. Chain of flux qubits with intervening dc SQUIDs arranged to provide both variable nearest-neighbor coupling and qubit readout.

This work was supported by the Air Force Office of Scientific Research under Grant No. F49-620-02-1-0295, the Army Research Office under Grant Nos. DAAD-19-02-1-0187 and P-43385-PH-QC, and the National Science Foundation under Grant No. EIA-020-5641. F.K.W. acknowledges travel support from Deutsche Forschungsgemeinschaft within Sonderforschungsbereich 631.

[1] A Quantum Information Science and Technology Roadmap Website, http://qist.lanl.gov

[2] Y. Nakamura, Yu. A. Pashkin, and J. S. Tsai, Nature (London) **398**, 786 (1999).

[3] D. Vion, A. Aassime, A. Cottet, P. Joyez, H. Pothier, C. Urbina, D. Esteve, and M. H. Devoret, Science **296**, 286 (2002).

[4] T. P. Orlando, J. E. Mooij, L. Tian, C. H. van der Wal, L. S. Levitov, S. Lloyd, and J. J. Mazo, Phys. Rev. B **60**, 15398 (1999).

[5] J. R. Friedman, V. Patel, W. Chen, S. K. Tolpygo, and J. E. Lukens, Nature (London) **46**, 43 (2000).

[6] C. H. van der Wal, A. C. J. ter Haar, F. K. Wilhelm, R. N. Schouten, C. J. P. M. Harmans, T. P. Orlando, S. Lloyd, and J. E. Mooij, Science **290**, 773 (2000).

[7] J. M. Martinis, S. Nam, J. Aumentado, and C. Urbina, Phys. Rev. Lett. **89**, 117901 (2002).

[8] A. Shnirman, G. Schön, and Z. Hermon, Phys. Rev. Lett. **79**, 2371 (1997).

[9] J. B. Majer *et al.*, cond-mat/0308192 (unpublished).

[10] T. Yamamoto, Yu. A. Pashkin, O. Astafiev, Y. Nakamura, and J. S. Tsai, Nature (London) **425**, 941 (2003).

[11] F. W. Strauch, P. R. Johnson, A. J. Dragt, C. J. Lobb, J. R. Anderson, and F. C. Wellstood, Phys. Rev. Lett. **91**, 167005 (2003).

[12] D. V. Averin and C. Bruder, Phys. Rev. Lett. **91**, 057003 (2003).

[13] J. E. Mooij, T. P. Orlando, L. Levitov, L. Tian, C. H. van der Wal, and S. Lloyd, Science **285**, 1036 (1999).

[14] J. Clarke, T. L. Robertson, B. L. T. Plourde, A. García-Martínez, P. A. Reichardt, D. J. Van Harlingen, B. Chesca, R. Kleiner, Y. Makhlin, G. Schön, A. Shnirman, and F. K. Wilhelm, Phys. Scr., T **102**, 173 (2002).

[15] V. Lefevre-Seguin *et al.*, Phys. Rev. B **46**, 5507 (1992).

[16] I. Chiorescu, Y. Nakamura,C. J. P. M. Harmans, and J. E. Mooij, Science **299**, 1869 (2003).

[17] C. Hilbert and J. Clarke, J. Low Temp. Phys. **61**, 237 (1985).

[18] F. K. Wilhelm, M. J. Storcz, C. H. van der Wal, C. J. P. M. Harmans, and J. E. Mooij, Adv. Solid State Phys. **43**, 763 (2003).

[19] A. Barenco, C. H. Bennett, R. Cleve, D. P. DiVincenzo, N. Margolus, P. Shor, T. Sleator, J. A. Smolin, and H. Weinfurter, Phys. Rev. A **52**, 3457 (1995).

[20] J. Zhang, J. Vala, S. Sastry, and K. B. Whaley, Phys. Rev. A **67**, 042313 (2003).

[21] Y. Makhlin, Quantum Inf. Process. **1**, 243 (2002).